Author(s): Tuovinen, R.; Pavlyukh, Y.; Perfetto, E.; Stefanucci, G.

Title: Time-Linear Quantum Transport Simulations with Correlated Nonequilibrium Green's
Functions

Year: 2023

Version: Published version

Time-Linear Quantum Transport Simulations with Correlated Nonequilibrium Green's Functions

R. Tuovinen[1,2] Y. Pavlyukh[3] E. Perfetto[4,5] and G. Stefanucci[4,5]

[1]*QTF Centre of Excellence, Department of Physics, University of Helsinki, Helsinki, P.O. Box 64, 00014, Finland*
[2]*Department of Physics, Nanoscience Center, University of Jyväskylä, Jyväskylä, P.O. Box 35, 40014, Finland*
[3]*Institute of Theoretical Physics, Faculty of Fundamental Problems of Technology, Wroclaw University of Science and Technology, 50-370 Wroclaw, Poland*
[4]*Dipartimento di Fisica, Università di Roma Tor Vergata, Via della Ricerca Scientifica 1, 00133 Rome, Italy*
[5]*INFN, Sezione di Roma Tor Vergata, Via della Ricerca Scientifica 1, 00133 Rome, Italy*

We present a time-linear scaling method to simulate open and correlated quantum systems out of equilibrium. The method inherits from many-body perturbation theory the possibility to choose selectively the most relevant scattering processes in the dynamics, thereby paving the way to the real-time characterization of correlated ultrafast phenomena in quantum transport. The open system dynamics is described in terms of an "embedding correlator" from which the time-dependent current can be calculated using the Meir-Wingreen formula. We show how to efficiently implement our approach through a simple grafting into recently proposed time-linear Green's function methods for closed systems. Electron-electron and electron-phonon interactions can be treated on equal footing while preserving all fundamental conservation laws.

Introduction.—Few systems in nature are in equilibrium. Behind the facade of, e.g., calm and stationary transport, the electrical and heat currents run violently. Such out-of-equilibrium dynamics bridges fields like quantum transport and optics [1,2], atomic and molecular physics [3,4], spectroscopy in solids [5–7], and cavity materials engineering [8–10]. Recent progress in state-of-the-art time-resolved pump-probe spectroscopy and transport measurements has pushed the temporal resolution down to the femtosecond timescale [11–15]. Inherently, the associated phenomena are time-dependent; the complex many-body systems are far from equilibrium, with no guarantee of instantly relaxing to stationary states.

The theory of quantum transport began with the pioneering works of Landauer and Büttiker [16–18] and became a mature field after the works of Meir, Wingreen, and Jauho [19,20], who provided a general formula for the time-dependent current through correlated junctions in terms of nonequilibrium Green's functions (NEGFs). The NEGF is an *ab initio* method suitable to deal with both bosonic and fermionic interacting particles, in and out of equilibrium [21–23]. Nonetheless, the ability to harness the full power of the Meir-Wingreen formula [19] is hampered by the underlying two-time structure of the NEGF, a feature that makes real-time simulations computationally challenging.

In this Letter, we present a time-linear scaling NEGF theory for "open" and "correlated" quantum systems. The resulting method is strikingly simple, with ordinary differential equations (ODEs) only. Correlation effects originating from different scattering mechanisms are included through a proper selection of Feynman diagrams, and all fundamental conservation laws are preserved. The Meir-Wingreen formula is rewritten in terms of an "embedding correlator" that allows for evaluating the time-dependent current at a "time-linear" cost. We use the method to study transport of electron-hole pairs, highlighting the pivotal role of correlations in capturing velocity renormalizations and decoherence mechanisms.

Kadanoff-Baym equations for open systems.—We consider a finite quantum system, be it a molecule or a nanostructure, with one-electron integrals $h_{ij}(t)$ and two-electron integrals v_{ijmn} in some orthonormal one-particle basis of dimension N_{sys}; see Fig. 1. The time dependence of $h_{ij}(t) = h_{ij}^0 + \langle i|V_{gate}(t) + \hat{\boldsymbol{d}} \cdot \boldsymbol{E}_{pulse}(t)|j\rangle$ is due to a time-dependent gate voltage $V_{gate}(t)$ and to a possible laser pulse
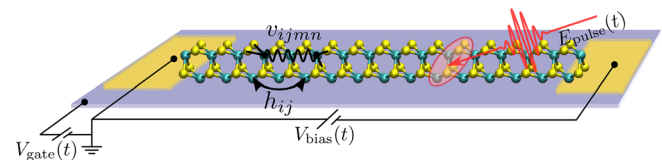

FIG. 1. Quantum transport setup. A nanowire (finite quantum system) is contacted to left ($\alpha = L$) and right ($\alpha = R$) electrodes and lies over a substrate (or gate electrode) $\alpha = $ gate. The nanowire is driven out of equilibrium by time-dependent voltages $V_\alpha(t)$ [$V_{bias} = V_L - V_R$] and laser pulses $E_{pulse}(t)$.

$E_{\mathrm{pulse}}(t)$ coupled to the electronic dipole operator $\hat{\boldsymbol{d}}$. The system is said to be "open" if it is in contact with electronic reservoirs with which it can exchange particles and hence energy. This is the typical quantum transport setup, the finite system being the junction and the electronic reservoirs being the electrodes. Neglecting correlation effects in the electrodes and between the electrodes and the system, the Green's function $G_{ij}(z, z')$ with times z, z' on the Keldysh contour C satisfies the equation of motion (EOM) (in the $N_{\mathrm{sys}} \times N_{\mathrm{sys}}$ matrix form) [20,22,24–26]

$$\left[\mathrm{i}\frac{d}{dz} - h^e(z) \right] G(z, z') = \delta(z, z') + \int_C d\bar{z} [\Sigma_c(z, \bar{z}) + \Sigma_{\mathrm{em}}(z, \bar{z})] G(\bar{z}, z'). \quad (1)$$

In Eq. (1) $h^e_{ij}(z) = h_{ij}(z) + V^{\mathrm{HF}}_{ij}(z)$ is the one-electron Hamiltonian properly renormalized by the Hartree-Fock (HF) potential $V^{\mathrm{HF}}_{ij}(z) = -i \sum_{mn} (v_{imnj} - v_{imjn}) G_{nm}(z, z^+)$, Σ_c is the correlation self-energy due to electron-electron interactions, and Σ_{em} is the embedding self-energy accounting for all virtual processes where an electron from orbital i leaves the system to occupy some energy level in one of the electrodes and thereafter moves back to the system in orbital j.

The Kadanoff-Baym equations (KBEs) for the open system follow from Eq. (1) by choosing the times z and z' on different branches of the Keldysh contour [22]. In particular the EOM for the $N_{\mathrm{sys}} \times N_{\mathrm{sys}}$ electronic density matrix $\rho(t) = -iG(z, z^+) = -iG^<(t, t)$ can easily be derived by subtracting Eq. (1) from its adjoint and then setting $z = t$ on the forward branch and $z' = t$ on the backward branch:

$$i\frac{d}{dt}\rho(t) = [h^e(t)\rho(t) - iI_c(t) - iI_{\mathrm{em}}(t)] - \mathrm{H.c.} \quad (2)$$

The collision integral I_c is the convolution between the correlation self-energy and the Green's function G, whereas the embedding integral I_{em}, the main focus of this work, is the convolution between the embedding self-energy and G. For $I_{\mathrm{em}} = 0$ the system is closed (no electrodes) and the KBEs have been implemented in a number of works using different approximations to Σ_c; these include the second Born [27,28], the GW and T matrix [29–32], the Fan-Migdal [33,34], and approximations based on the nonequilibrium dynamical mean-field theory [35–38]. KBE studies of open systems are less numerous [25,26,31]. In all cases, the unfavorable $O(N_t^3)$ scaling with the number of time steps N_t limits the KBE, and hence the possibility of studying ultrafast correlated dynamics, to relatively small systems, although promising progress has been recently achieved [32,39–41].

Generalized Kadanoff-Baym ansatz.—For any given correlation self-energy the direct solution of the EOM

for the density matrix [see Eq. (2)] is computationally less complex than solving the KBE and opens the door to a wealth of nonequilibrium phenomena [42]. To date the most efficient way to make the collision integral a functional of ρ is the generalized Kadanoff-Baym ansatz (GKBA) [43]

$$G^{\lessgtr}(t, t') = -G^R(t, t')\rho^{\lessgtr}(t') + \rho^{\lessgtr}(t)G^A(t, t'), \quad (3)$$

with $G^{R/A}$ the $N_{\mathrm{sys}} \times N_{\mathrm{sys}}$ retarded or advanced quasiparticle propagators, $\rho^> = \rho - 1$ and $\rho^< = \rho$. The GKBA respects the causal structure and it preserves all fundamental conservation laws for Φ-derivable approximations [44] to Σ_c [45]. In "closed" systems the GKBA EOM can be exactly reformulated in terms of a coupled set of ODEs [46,47] for several major approximations to Σ_c, the most notable being the GW and T matrix [46–48], the GW and T matrix plus exchange [49,50], the Fan-Migdal [45], and the doubly screened $G\tilde{W}$ [51]. In essence, the idea is to introduce high-order correlators $\mathcal{G}^{a=1,\ldots,n}(t)$ ($\mathcal{G}^1 = \rho$), write $I_c[\{\mathcal{G}^a\}]$ as a functional of them, and solve the coupled EOMs $i(d/dt)\mathcal{G}^a = \mathcal{I}^a[\{\mathcal{G}^a\}]$ [$\mathcal{I}^1 = (h^e\rho - iI_c) - \mathrm{H.c.}$]. For all aforementioned methods the system of ODEs can be closed using a relatively few number of correlators (the highest number being $n = 7$ in $G\tilde{W}$). Extending the ODE formulation to open systems would enable performing time-linear [$O(N_t)$ scaling] NEGF simulations of correlated junctions and hence studying, e.g., the formation of Kondo singlets [52], blocking dynamics of polarons [53,54], bistability and hysteresis [55,56], phonon dynamics and heating [57–60], nonconservative dynamics [61–64], molecular electroluminescence [1], and the transport and optical response of junctions under periodic drivings [65,66]; see also Ref. [67] for a recent review.

Below we show that the set of ODEs for closed systems can be coupled to one more ODE for the embedding correlator $\mathcal{G}^{\mathrm{em}}$ to effectively open the system, thus providing a time-linear method to solve Eq. (2). Equation (2) was originally investigated using the integral (convolution) form of the collision and embedding integrals in Refs. [68–71]. It was emphasized therein that the GKBA propagators $G^{R/A}$ chosen for closed-system simulations need to be modified. This change affects all other ODEs in an extremely elegant way while preserving the overall computational complexity.

Time-linear method.—Let Σ_α be the embedding self-energy of electrode $\alpha = 1, \ldots, N_{\mathrm{leads}}$, hence $\Sigma_{\mathrm{em}} = \sum_\alpha \Sigma_\alpha$. In the so-called wide-band limit approximation (WBLA) [72], the retarded and lesser components read [22,73,74]

$$\Sigma_\alpha^R(t, t') = -\frac{i}{2}s_\alpha^2(t)\delta(t, t')\Gamma_\alpha, \quad (4a)$$

$$\Sigma_\alpha^<(t, t') = is_\alpha(t)s_\alpha(t')e^{-i\phi_\alpha(t,t')} \int \frac{d\omega}{2\pi} f(\omega - \mu)e^{-i\omega(t-t')}\Gamma_\alpha, \quad (4b)$$

where $s_\alpha(t)$ is the switch-on function for the contact between the system and electrode α, Γ_α is the $N_{sys} \times N_{sys}$ quasiparticle line-width matrix due to electrode α, $\phi_\alpha(t, t') \equiv \int_{t'}^{t} d\bar{t} V_\alpha(\bar{t})$ is the accumulated phase due to the time-dependent voltage V_α [77], and $f(\omega - \mu) = 1/(e^{\beta(\omega-\mu)} + 1)$ is the Fermi function at inverse temperature β and chemical potential μ. The matrix elements $\Gamma_{\alpha,ij} = 2\pi \sum_k T_{ik\alpha} \delta(\mu - \epsilon_{k\alpha}) T_{k\alpha j}$ can be calculated from the transition amplitudes $T_{k\alpha j} = T_{jk\alpha}^*$ from orbital j to level k in electrode α having the energy dispersion $\epsilon_{k\alpha}$. The exact form of the embedding integral is then

$$I_{em}(t) = \sum_\alpha I_\alpha(t) = \int d\bar{t} \Sigma_{em}^<(t, \bar{t}) G^A(\bar{t}, t) + \frac{1}{2}\Gamma(t)\rho(t), \quad (5)$$

with $\Gamma(t) \equiv \sum_\alpha s_\alpha^2(t)\Gamma_\alpha$. In Ref. [68] it was shown that the mean-field approximation of Eq. (2), i.e., $I_c = 0$, is exactly reproduced in GKBA provided that

$$G^R(t, t') = -i\theta(t - t')Te^{-i\int_{t'}^{t} d\bar{t}(h^e(\bar{t}) - i\Gamma(\bar{t})/2)}, \quad (6)$$

and $G^A(t', t) = [G^R(t, t')]^\dagger$. Equation (6) reduces to the propagator of closed systems for $\Gamma = 0$. In open systems, however, setting $\Gamma = 0$ is utterly inadequate as no steady state would ever be attained. Beyond the mean-field approximation we close Eq. (2) using the GKBA with propagators as in Eq. (6) [78].

To construct the time-linear method we use an efficient pole expansion (PE) scheme for the Fermi function [79] $f(\omega) = \frac{1}{2} - \sum_l \eta_l\{[1/(\beta\omega + i\zeta_l)] + [1/(\beta\omega - i\zeta_l)]\}$, $\text{Re}[\zeta_l] > 0$, to rewrite the lesser self-energy for $t > t'$ as $\Sigma_\alpha^<(t, t') = (i/2)s_\alpha^2(t)\delta(t - t')\Gamma_\alpha - s_\alpha(t) \sum_l (\eta_l/\beta)F_{l\alpha}(t, t')\Gamma_\alpha$ with

$$F_{l\alpha}(t, t') = s_\alpha(t')e^{-i\phi_\alpha(t,t')}e^{-i(\mu - i\frac{\zeta_l}{\beta})(t-t')}. \quad (7)$$

Inserting the result into Eq. (5) the EOM Eq. (2) for the density matrix becomes

$$i\frac{d}{dt}\rho = \left(h_{eff}^e\rho + \frac{i}{4}\Gamma + i\sum_{l\alpha} s_\alpha \frac{\eta_l}{\beta}\Gamma_\alpha \mathcal{G}_{l\alpha}^{em} - iI_c\right) - \text{H.c.}, \quad (8)$$

where $h_{eff}^e(t) \equiv h^e(t) - i\Gamma(t)/2$ is the effective (non-self-adjoint) mean-field Hamiltonian and $\mathcal{G}_{l\alpha}^{em}(t) \equiv \int d\bar{t} F_{l\alpha}(t, \bar{t}) G^A(\bar{t}, t)$ is the $N_{sys} \times N_{sys}$ embedding correlator. Taking into account the explicit expressions in Eqs. (6) and (7) we find

$$i\frac{d}{dt}\mathcal{G}_{l\alpha}^{em}(t) = -s_\alpha(t) - \mathcal{G}_{l\alpha}^{em}(t)\left(h_{eff}^{e\dagger}(t) - V_\alpha(t) - \mu + i\frac{\zeta_l}{\beta}\right). \quad (9)$$

Equations (8) and (9), together with the ODEs for I_c, form a coupled system of ODEs for correlated real-time simulations of open systems. This time-linear method becomes similar to

the one of Refs. [80–85] for $I_c = 0$. The scaling with the system size of Eq. (9) grows like $N_{sys}^3 \times N_p \times N_{leads}$ where N_p is the number of poles for the expansion of $f(\omega)$ [74].

An alternative time-linear method can be constructed from the spectral decomposition (SD) of the embedding self-energy $\Sigma_\alpha(z, z') = s_\alpha(z)s_\alpha(z') \sum_k T_{ik\alpha}g_{k\alpha}(z, z')T_{k\alpha j}$, where $g_{k\alpha}$ is the Green's function of the isolated electrode. In this case, one would rewrite the embedding integral as $I_{em,ij} = \sum_{k\alpha} T_{ik\alpha} \widetilde{\mathcal{G}}_{k\alpha j}^{em}$ and derive an ODE for the scalar quantities $\widetilde{\mathcal{G}}_{k\alpha j}^{em} = \sum_m \int d\bar{t}[g_{k\alpha}^R(t, \bar{t})T_{k\alpha m}G_{mj}^<(\bar{t}, t) + g_{k\alpha}^<(t, \bar{t})T_{k\alpha m}G_{mj}^A(\bar{t}, t)]$ using the GKBA for the lesser Green's function. The scaling with the system size of the scalar ODE for all $\widetilde{\mathcal{G}}_{k\alpha j}^{em}$ grows like $N_{sys}^2 \times N_k \times N_{leads}$ [74], where N_k is the number of k points needed for the discretization. The SD scheme is ill-advised for the following reasons. If the electrodes are not wide band then the calculation of the mean-field propagator scales cubically in time; any other approximation to G^R, including Eq. (6), would be inconsistent and could even lead to unphysical time evolutions, e.g., no steady states for constant voltages. If the electrodes are wide band then N_k could be orders of magnitude larger than $N_{sys} \times N_p$ to achieve convergence; hence, $N_{sys}^2 \times N_k \gg N_{sys}^3 \times N_p$. This statement is proven numerically below; see also Supplemental Material [74].

The quasiparticle broadening Γ in the propagators [see Eq. (6)] is only responsible for a minor change in the ODEs for the high-order correlators of closed systems. We focus here on the T-matrix approximation in the particle-hole channel (T^{ph}) as T^{ph} simulations of open systems are reported below; similar arguments apply to all other approximations in Ref. [51]. The collision integral is $I_{c,ij} = -i \sum_{lmn} v_{inml}\mathcal{G}_{lmjn}^c$ where $\mathcal{G}_{lmjn}^c = -\langle \hat{d}_j^\dagger \hat{d}_n^\dagger \hat{d}_l \hat{d}_m \rangle_c$ is the correlated part of the equal-time two-particle Green's function [22]. Following Refs. [49,50], we construct the matrices in the two-electron space $\mathcal{G}_{ij}^c(t) \equiv \mathcal{G}_{imjn}^c(t)$, $v_{ij} \equiv v_{imnj}$ and $\rho_{ij}^\lessgtr \equiv \rho_{ij}^\lessgtr \rho_{mn}^\gtrless$ (boldface letters are used to distinguish them from matrices in one-electron space). The only difference in the derivation of the EOM for $\mathcal{G}$ of closed systems [49,50] comes from the fact that the EOM for the propagator contains h_{eff}^e instead of h^e. The final result is therefore

$$i\frac{d}{dt}\mathcal{G}^c = (\rho^< v\rho^> + (h_{eff}^e + \rho^\Delta v)\mathcal{G}^c) - \text{H.c.}, \quad (10)$$

where $\rho^\Delta = \rho^> - \rho^<$ and $h_{eff,ij}^e \equiv h_{eff,ij}^e \delta_{mn} - \delta_{ij} h_{eff,nm}^{e\dagger}$. The solution of the coupled ODEs for ρ, $\mathcal{G}^{em}$, and $\mathcal{G}^c$ yields the time-dependent evolution of open systems in the T^{ph} approximation. Similarly, one can show that all the 2^{12} NEGF methods of Ref. [51] are only affected by the replacement $h^e \to h_{eff}^e$. The addition of I_{em} in the EOM for

ρ, along with the propagation of the embedding correlator according to Eq. (9), allows for studying open systems for a large number of NEGF methods. These include methods to deal with the electron-phonon interaction as well [45]. Noteworthily, all NEGF methods in Ref. [51] guarantee the satisfaction of fundamental conservation laws like the continuity equation and the energy balance.

Charge current.—Charge distributions, local currents, local moments, etc., can be extracted from the one-particle density matrix ρ. Information on the electron-hole pair correlation function is carried by the T^{ph} correlator $\mathcal{G}^c$. The embedding correlator $\mathcal{G}^{\mathrm{em}}$ is instead crucial for calculating the time-dependent current $J_\alpha(t)$ at the interface between the system and electrode α. This current is given by the Meir-Wingreen formula [19] and it can be written as the contribution of the α electrode to the embedding integral [20,22,24] [see Eq. (5)] $J_\alpha(t) = 2\mathrm{ReTr}[I_\alpha(t)]$. Expressing the embedding self-energy in terms of $\mathcal{G}^{\mathrm{em}}$ we find

$$J_\alpha(t) = 2s_\alpha(t)\mathrm{ReTr}\left\{\Gamma_\alpha\left[s_\alpha(t)\frac{2\rho(t)-1}{4} - \sum_l \frac{\eta_l}{\beta}\mathcal{G}_{l\alpha}^{\mathrm{em}}(t)\right]\right\}. \tag{11}$$

Satisfaction of the continuity equation implies $\mathrm{CE} \equiv (d/dt)\mathrm{Tr}[\rho] + \sum_\alpha J_\alpha = 0$.

Spectral decomposition vs pole expansion.—We first study a two-level molecule coupled to two one-dimensional tight-binding electrodes. We set $h_{11} = h_{22} = 0$, $h_{12} = h_{21} = -T/2$ and measure all energies in units of $T > 0$. We consider an interaction $v_{ijmn} = v_{ij}\delta_{in}\delta_{jm}$ with $v_{11} = v_{22} = 1$ and $v_{12} = v_{21} = 0.5$. The chemical potential is fixed at the middle of the HF gap of the uncontacted system, in our case $\mu = 1$, and the inverse temperature is $\beta = 100$. The electrodes are parameterized by on-site and hopping energies $a_\alpha = \mu$ (half-filled electrodes), $b_\alpha = -8$, respectively, the energy dispersion thus taking the form $\epsilon_{k\alpha} = a_\alpha - 2|b_\alpha|\cos[\pi k/(N_k + 1)]$, with N_k the number of discretized k points. The left and right electrodes are coupled to the first and second molecular levels, respectively, with transition amplitude $T_\alpha = -0.2$, $\alpha = L, R$. As $T_\alpha \ll b_\alpha$ the WBLA is accurate and one finds $\Gamma_{L,ij} = \delta_{i1}\delta_{j1}\gamma_L$ and $\Gamma_{R,ij} = \delta_{i2}\delta_{j2}\gamma_R$ with $\gamma_\alpha = 2T_\alpha^2/|b_\alpha| = 0.01$.

In Fig. 2 we present time-dependent HF results for the occupation of the first level [panel (a)] and the current at the left interface [panel (b)]. We adiabatically switch on the contacts between the molecule and the electrodes for $t < 0$ with a "sine-squared" switch-on function [86], and then drive the system away from equilibrium with a constant bias $V_L = T/2$, $V_R = 0$ for $t \geq 0$ (hence $V_{\mathrm{gate}} = 0$, $E_{\mathrm{pulse}} = 0$, $V_{\mathrm{bias}} = V_L - V_R$). The time-linear PE and SD schemes perform similarly at convergence, as they should. However, within the time frame of the simulation, $N_k = 1000$ k points are needed to converge the SD scheme, against only $N_p = 20$ poles needed to converge the PE
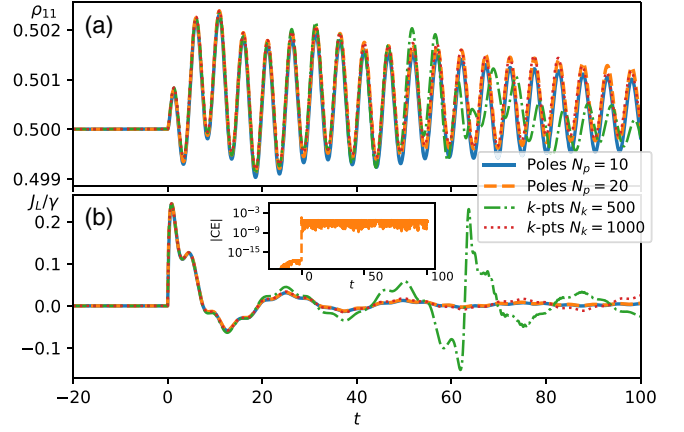

FIG. 2. Dynamics of the two-level molecule contacted to a left and right electrodes. Occupation of the first level (a) and current at the left interface (b) using the SD (k points N_k) and PE (poles N_p) schemes. The inset in panel (b) shows the continuity equation $\mathrm{CE} = (d/dt)\mathrm{Tr}[\rho] + \sum_\alpha J_\alpha$. Energies in units of T and time in units of $1/T$.

scheme. Furthermore, the convergence with N_p is independent of the maximum simulation time whereas N_k must grow linearly with it for otherwise finite size effects, as those visible for $N_k = 500$ at time $t \simeq 50$, take place. Steady values are attained on a timescale of a few $1/\gamma_a$ time units [74]. The inset in Fig. 2(b) shows that the continuity equation is satisfied with high accuracy.

Correlated electron-hole transport.—Transport of correlated electron holes (eh) is a fundamental process in photovoltaic junctions [87,88]. We study the relaxation of a suddenly created eh in a two-band direct gap one-dimensional semiconductor coupled to WBLA electrodes. The Hamiltonian of the system reads $\hat{H} = \sum_{ij\nu} h_{ij\nu}\hat{d}_{i\nu}^\dagger\hat{d}_{j\nu} + U\sum_i \hat{n}_{iv}\hat{n}_{ic}$, where $\hat{d}_{i\nu}$ destroys an electron in the ith valence ($\nu = v$) or conduction ($\nu = c$) orbital, and $\hat{n}_{i\nu} \equiv \hat{d}_{i\nu}^\dagger\hat{d}_{i\nu}$ is the orbital occupation. The one-electron integrals are $h_{iiv} = -\epsilon_0 < 0$, $h_{iic} = \epsilon_0 - U$ on site and $h_{ijv} = -h_{ijc} = T > 0$ for nearest neighbors [89]. In equilibrium the HF gap is $\Delta = 2(\epsilon_0 - 2T)$. The left and right electrodes are coupled to the left- and right-most orbitals, respectively, with tunneling strength γ_α independent of α. Henceforth all energies are measured in units of $\Delta/2$; we set $\epsilon_0 = 4.5$, $T = 1.75$, $\gamma_\alpha = 0.1$ and work at inverse temperature $\beta = 100$. The equilibrium chemical potential is set in the middle of the HF gap of the uncontacted system.

At time $t = 0$ we suddenly couple the system to the electrodes and create an eh excitation at the left-most orbitals, hence $\rho_{iv,iv}(0) = (1 - \delta_{i1})$ and $\rho_{ic,ic}(0) = \delta_{i1}$. In Figs. 3(a) and 3(b), we show the current at the right interface in two different many-body methods, i.e., HF and T^{ph}, and for two values $U = 1, 2$ of the eh attraction. The results indicate that (i) the velocity of the eh wave packet is faster in HF than T^{ph} (each spike corresponds to an eh
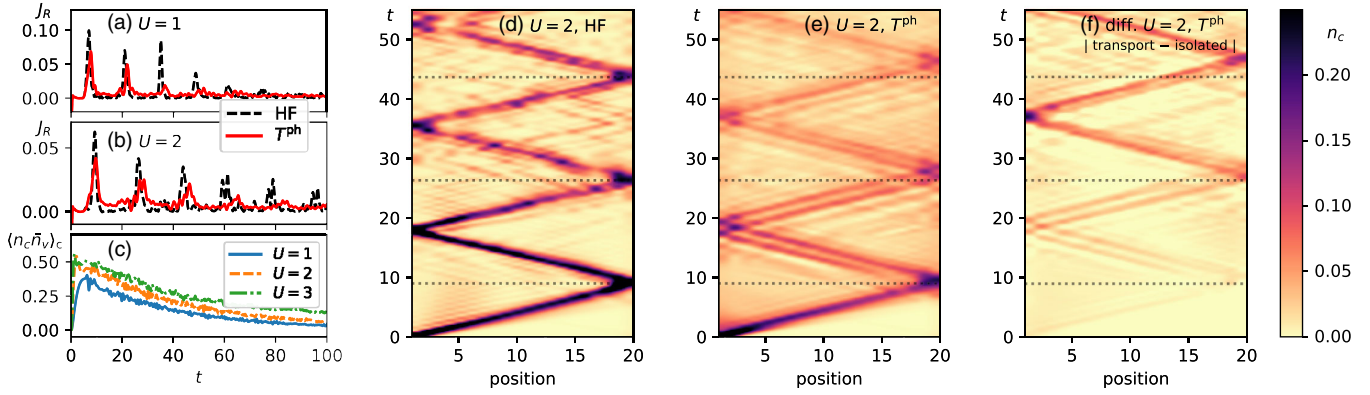
FIG. 3.   Dynamics of an electron-hole pair in a one-dimensional semiconductor junction with $N = 20$ cells. (a),(b) Time-dependent current at the right interface in HF (dashed) and T^{ph} (solid) for $U = 1$ (a) and $U = 2$ (b). (c) Correlated part of the total number of eh pairs for different interaction strengths. (d),(e) Conduction occupations (color map) versus time (vertical axis) and cell position (horizontal axis) in HF (d) and T^{ph} (e). (f) Difference of panel (e) to a situation without electrodes. The dashed lines are guides to the eye.

bouncing at the right interface), and (ii) the HF dynamics is coherent, the wave packet travelling almost undisturbed, whereas in T^{ph} correlations are responsible for a fast decoherence and wave packet spreading. The slower velocity in T^{ph} is rationalized in Fig. 3(c) where we plot the correlated part of the total number of eh pairs: $\sum_i \langle (1 - \hat{n}_{iv}) \hat{n}_{ic} \rangle_c = -\sum_i \mathcal{G}^c_{icivivic}$. The buildup of correlations is almost instantaneous. The initially uncorrelated eh pair binds and becomes heavier, thus reducing the propagation speed. The observed decay at longer times is due to electron and hole tunneling into the electrodes; at the steady state about 10^{-2} conduction electrons and valence holes remain in the system (not shown). Both decoherence and velocity reduction are well visible in Figs. 3(d) and 3(e) where we display the color plot of the conduction occupations $n_{ic}(t) = \rho_{ic,ic}(t)$ in HF and T^{ph} for $U = 2$. In T^{ph} the *eh* wave packet loses coherence and spreads after bouncing back and forth a few times. In Fig. 3(f) we analyze the effect of the electrodes by showing the difference between the open and closed system dynamics. In the open system the amplitude of the wave packet and the localization of the charge decreases faster than in the isolated system.

In conclusion, we put forward a time-linear approach to study the correlated dynamics of open systems with a large number of NEGF methods. Our work empowers the Meir-Wingreen formula allowing its use in contexts and/or for levels of approximation that were previously unattainable in practice. The ODE formulation lends itself to parallel computation, adaptive time-stepping implementations and restart protocols, thus opening new avenues for the *ab initio* description of time-dependent quantum transport phenomena.

[1] K. Miwa, H. Imada, M. Imai-Imada, K. Kimura, M. Galperin, and Y. Kim, Nano Lett. **19**, 2803 (2019).

[2] H. Hübener, U. De Giovannini, C. Schäfer, J. Andberger, M. Ruggenthaler, J. Faist, and A. Rubio, Nat. Mater. **20**, 438 (2021).

[3] M. Ruggenthaler, N. Tancogne-Dejean, J. Flick, H. Appel, and A. Rubio, Nat. Rev. Chem. **2**, 0118 (2018).

[4] E. P. Månsson, S. Latini, F. Covito, V. Wanie, M. Galli, E. Perfetto, G. Stefanucci, H. Hübener, U. De Giovannini, M. C. Castrovilli, A. Trabattoni, F. Frassetto, L. Poletto, J. B. Greenwood, F. Légaré, M. Nisoli, A. Rubio, and F. Calegari, Commun. Chem. **4**, 73 (2021).

[5] M. Buzzi *et al.*, Phys. Rev. X **10**, 031028 (2020).

[6] M. Dendzik *et al.*, Phys. Rev. Lett. **125**, 096401 (2020).

[7] D. Nicoletti, M. Buzzi, M. Fechner, P. E. Dolgirev, M. H. Michael, J. B. Curtis, E. Demler, G. D. Gu, and A. Cavalleri, Proc. Natl. Acad. Sci. U.S.A. **119**, e2211670119 (2022).

[8] S. Latini, D. Shin, S. A. Sato, C. Schäfer, U. D. Giovannini, H. Hübener, and A. Rubio, Proc. Natl. Acad. Sci. U.S.A. **118**, e2105618118 (2021).

[9] C. Bao, P. Tang, D. Sun, and S. Zhou, Nat. Rev. Phys. **4**, 33 (2022).

[10] F. Schlawin, D. M. Kennes, and M. A. Sentef, Appl. Phys. Rev. **9**, 011312 (2022).

[11] J. W. McIver, B. Schulte, F.-U. Stein, T. Matsuyama, G. Jotzu, G. Meier, and A. Cavalleri, Nat. Phys. **16**, 38 (2020).

[12] J. Sung, C. Schnedermann, L. Ni, A. Sadhanala, R. Y. S. Chen, C. Cho, L. Priest, J. M. Lim, H.-K. Kim,

B. Monserrat, P. Kukura, and A. Rao, Nat. Phys. **16**, 171 (2020).

[13] A. De Sio, E. Sommer, X. T. Nguyen, L. Groß, D. Popović, B. T. Nebgen, S. Fernandez-Alberti, S. Pittalis, C. A. Rozzi, E. Molinari, E. Mena-Osteritz, P. Bäuerle, T. Frauenheim, S. Tretiak, and C. Lienau, Nat. Nanotechnol. **16**, 63 (2021).

[14] M. Abdo, S. Sheng, S. Rolf-Pissarczyk, L. Arnhold, J. A. J. Burgess, M. Isobe, L. Malavolti, and S. Loth, ACS Photonics **8**, 702 (2021).

[15] A. Niedermayr, M. Volkov, S. A. Sato, N. Hartmann, Z. Schumacher, S. Neb, A. Rubio, L. Gallmann, and U. Keller, Phys. Rev. X **12**, 021045 (2022).

[16] R. Landauer, IBM J. Res. Dev. **1**, 233 (1957).

[17] M. Büttiker, Y. Imry, R. Landauer, and S. Pinhas, Phys. Rev. B **31**, 6207 (1985).

[18] M. Büttiker, Phys. Rev. Lett. **57**, 1761 (1986).

[19] Y. Meir and N. S. Wingreen, Phys. Rev. Lett. **68**, 2512 (1992).

[20] A.-P. Jauho, N. S. Wingreen, and Y. Meir, Phys. Rev. B **50**, 5528 (1994).

[21] P. Danielewicz, Ann. Phys. (N.Y.) **152**, 239 (1984).

[22] G. Stefanucci and R. van Leeuwen, *Nonequilibrium Many-Body Theory of Quantum Systems: A Modern Introduction* (Cambridge University Press, Cambridge, 2013).

[23] K. Balzer and M. Bonitz, *Nonequilibrium Green's Functions Approach to Inhomogeneous Systems* (Springer, New York, 2013).

[24] H. Haug and A.-P. Jauho, *Quantum Kinetics in Transport and Optics of Semiconductors* (Springer, New York, 2008).

[25] P. Myöhänen, A. Stan, G. Stefanucci, and R. van Leeuwen, Europhys. Lett. **84**, 67001 (2008).

[26] P. Myöhänen, A. Stan, G. Stefanucci, and R. van Leeuwen, Phys. Rev. B **80**, 115107 (2009).

[27] N. E. Dahlen and R. van Leeuwen, Phys. Rev. Lett. **98**, 153004 (2007).

[28] K. Balzer, S. Hermanns, and M. Bonitz, Europhys. Lett. **98**, 67002 (2012).

[29] M. Puig von Friesen, C. Verdozzi, and C.-O. Almbladh, Phys. Rev. Lett. **103**, 176404 (2009).

[30] A. Stan, N. E. Dahlen, and R. van Leeuwen, J. Chem. Phys. **130**, 224101 (2009).

[31] M. Puig von Friesen, C. Verdozzi, and C.-O. Almbladh, Phys. Rev. B **82**, 155108 (2010).

[32] M. Schüler, D. Golež, Y. Murakami, N. Bittner, A. Herrmann, H. U. Strand, P. Werner, and M. Eckstein, Comput. Phys. Commun. **257**, 107484 (2020).

[33] N. Säkkinen, Y. Peng, H. Appel, and R. van Leeuwen, J. Chem. Phys. **143**, 234102 (2015).

[34] M. Schüler, J. Berakdar, and Y. Pavlyukh, Phys. Rev. B **93**, 054303 (2016).

[35] J. K. Freericks, V. M. Turkowski, and V. Zlatić, Phys. Rev. Lett. **97**, 266408 (2006).

[36] H. Aoki, N. Tsuji, M. Eckstein, M. Kollar, T. Oka, and P. Werner, Rev. Mod. Phys. **86**, 779 (2014).

[37] H. U. R. Strand, M. Eckstein, and P. Werner, Phys. Rev. X **5**, 011038 (2015).

[38] D. Golež, L. Boehnke, H. U. R. Strand, M. Eckstein, and P. Werner, Phys. Rev. Lett. **118**, 246402 (2017).

[39] J. Kaye and D. Golež, SciPost Phys. **10**, 091 (2021).

[40] F. Meirinhos, M. Kajan, J. Kroha, and T. Bode, SciPost Phys. Core **5**, 030 (2022).

[41] X. Dong, E. Gull, and H. U. R. Strand, Phys. Rev. B **106**, 125153 (2022).

[42] E. Perfetto and G. Stefanucci, J. Phys. Condens. Matter **30**, 465901 (2018).

[43] P. Lipavský, V. Špička, and B. Velický, Phys. Rev. B **34**, 6933 (1986).

[44] G. Baym, Phys. Rev. **127**, 1391 (1962).

[45] D. Karlsson, R. van Leeuwen, Y. Pavlyukh, E. Perfetto, and G. Stefanucci, Phys. Rev. Lett. **127**, 036402 (2021).

[46] N. Schlünzen, J.-P. Joost, and M. Bonitz, Phys. Rev. Lett. **124**, 076601 (2020).

[47] J.-P. Joost, N. Schlünzen, and M. Bonitz, Phys. Rev. B **101**, 245101 (2020).

[48] E. Perfetto, Y. Pavlyukh, and G. Stefanucci, Phys. Rev. Lett. **128**, 016801 (2022).

[49] Y. Pavlyukh, E. Perfetto, and G. Stefanucci, Phys. Rev. B **104**, 035124 (2021).

[50] Y. Pavlyukh, E. Perfetto, D. Karlsson, R. van Leeuwen, and G. Stefanucci, Phys. Rev. B **105**, 125134 (2022).

[51] Y. Pavlyukh, E. Perfetto, and G. Stefanucci, Phys. Rev. B **106**, L201408 (2022).

[52] I. Krivenko, J. Kleinhenz, G. Cohen, and E. Gull, Phys. Rev. B **100**, 201104(R) (2019).

[53] K. F. Albrecht, A. Martin-Rodero, R. C. Monreal, L. Mühlbacher, and A. Levy Yeyati, Phys. Rev. B **87**, 085127 (2013).

[54] E. Y. Wilner, H. Wang, M. Thoss, and E. Rabani, Phys. Rev. B **89**, 205129 (2014).

[55] M. Galperin, M. A. Ratner, and A. Nitzan, Nano Lett. **5**, 125 (2005).

[56] E. Y. Wilner, H. Wang, G. Cohen, M. Thoss, and E. Rabani, Phys. Rev. B **88**, 045137 (2013).

[57] M. Galperin, M. A. Ratner, and A. Nitzan, J. Phys. Condens. Matter **19**, 103201 (2007).

[58] M. Galperin, A. Nitzan, and M. A. Ratner, Phys. Rev. B **75**, 155312 (2007).

[59] E. Y. Wilner, H. Wang, M. Thoss, and E. Rabani, Phys. Rev. B **90**, 115145 (2014).

[60] V. Rizzi, T. N. Todorov, J. J. Kohanoff, and A. A. Correa, Phys. Rev. B **93**, 024306 (2016).

[61] T. N. Todorov, J. Hoekstra, and A. P. Sutton, Phys. Rev. Lett. **86**, 3606 (2001).

[62] D. Dundas, E. J. McEniry, and T. N. Todorov, Nat. Nanotechnol. **4**, 99 (2009).

[63] N. Bode, S. V. Kusminskiy, R. Egger, and F. von Oppen, Phys. Rev. Lett. **107**, 036804 (2011).

[64] F. Chen, K. Miwa, and M. Galperin, J. Phys. Chem. A **123**, 693 (2019).

[65] G. Cabra, I. Franco, and M. Galperin, J. Chem. Phys. **152**, 094101 (2020).

[66] X. Zheng, Y. J. Yan, and M. Di Ventra, Phys. Rev. Lett. **111**, 086601 (2013).

[67] M. Ridley, N. W. Talarico, D. Karlsson, N. L. Gullo, and R. Tuovinen, J. Phys. A **55**, 273001 (2022).

[68] S. Latini, E. Perfetto, A.-M. Uimonen, R. van Leeuwen, and G. Stefanucci, Phys. Rev. B **89**, 075306 (2014).

[69] R. Tuovinen, D. Golež, M. Eckstein, and M. A. Sentef, Phys. Rev. B **102**, 115157 (2020).

[70] R. Tuovinen, R. van Leeuwen, E. Perfetto, and G. Stefanucci, J. Chem. Phys. **154**, 094104 (2021).

[71] R. Tuovinen, New J. Phys. **23**, 083024 (2021).

[72] As the GKBA performs poorly for narrow band electrodes [68] we only consider the WBLA.

[73] R. Tuovinen, E. Perfetto, G. Stefanucci, and R. van Leeuwen, Phys. Rev. B **89**, 085131 (2014).

[74] See Supplemental Material at http://link.aps.org/supplemental/10.1103/PhysRevLett.130.246301 for more detailed discussion, which includes Refs. [75,76].

[75] M. Ridley, A. MacKinnon, and L. Kantorovich, Phys. Rev. B **95**, 165440 (2017).

[76] G. Stefanucci, E. Perfetto, and M. Cini, Phys. Rev. B **78**, 075425 (2008).

[77] M. Ridley, A. MacKinnon, and L. Kantorovich, Phys. Rev. B **91**, 125433 (2015).

[78] More refined propagators can be considered, see Ref. [68], without affecting the overall computational scaling.

[79] J. Hu, R.-X. Xu, and Y. Yan, J. Chem. Phys. **133**, 101106 (2010).

[80] A. Croy and U. Saalmann, Phys. Rev. B **80**, 245311 (2009).

[81] X. Zheng, G. Chen, Y. Mo, S. Koo, H. Tian, C. Yam, and Y. Yan, J. Chem. Phys. **133**, 114101 (2010).

[82] Y. Zhang, S. Chen, and G. H. Chen, Phys. Rev. B **87**, 085110 (2013).

[83] Y. H. Kwok, H. Xie, C. Y. Yam, X. Zheng, and G. H. Chen, J. Chem. Phys. **139**, 224111 (2013).

[84] R. Wang, D. Hou, and X. Zheng, Phys. Rev. B **88**, 205126 (2013).

[85] Y. Kwok, G. Chen, and S. Mukamel, Nano Lett. **19**, 7006 (2019).

[86] D. Karlsson, R. van Leeuwen, E. Perfetto, and G. Stefanucci, Phys. Rev. B **98**, 115148 (2018).

[87] C. S. Ponseca, P. Chábera, J. Uhlig, P. Persson, and V. Sundström, Chem. Rev. **117**, 10940 (2017).

[88] E. Pastor, J.-S. Park, L. Steier, S. Kim, M. Grätzel, J. R. Durrant, A. Walsh, and A. A. Bakulin, Nat. Commun. **10**, 3962 (2019).

[89] E. Perfetto, D. Sangalli, A. Marini, and G. Stefanucci, Phys. Rev. Mater. **3**, 124601 (2019).